

Structural polymorphism in a tubercidin analogue of the DNA double helix

Lisa H. Pope ^a, Mark W. Shotton ^a, Trevor Forsyth ^{a,*}, Darren J. Hughes ^a,
Richard C. Denny ^b, Watson Fuller ^a

^a *Physics Department, Keele University, Staffordshire ST5 5BG, UK*

^b *Biophysics Section, Blackett Laboratory, Imperial College, London SW7 2BZ, UK*

Received 30 July 1997; revised 13 November 1997; accepted 17 November 1997

Abstract

A high-angle X-ray fibre diffraction study of a tubercidin analogue of the poly[d(A-T)] · poly[d(A-T)] DNA double helix has been carried out using station 7.2 at the Daresbury Laboratory synchrotron radiation source. The polymer has been studied for a wide range of salt strengths and hydration conditions and exhibits conformational polymorphism that is quite distinct from that observed for the unmodified polymer. The replacement of deoxyadenosine by deoxytubercidin in the polynucleotide causes only slight alterations to the structure of A-DNA, but significantly alters the structure of the B conformation. Additionally, the modified polymer does not, in any conditions yet identified, adopt the D conformation. In conditions which would normally favour the D conformation of poly[d(A-T)] · poly[d(A-T)], the modified polymer adopts an unusual conformation which is designated here as the K conformation. These observations are important for an understanding of major groove interactions involved in the stabilisation of particular DNA conformations and also more generally for an insight into the pharmacological activity of tubercidin which following its incorporation into nucleic acids may cause stereochemical distortions of the DNA double helix. © 1998 Elsevier Science B.V.

Keywords: Tubercidin; Deoxytubercidin; 7-Deazaadenine; DNA; DNA–drug interactions; High-angle X-ray fibre diffraction; Daresbury synchrotron radiation source (SRS)

1. Introduction

The cytotoxic antibiotic drug tubercidin (7-deazaadenosine) is the 7-deaza derivative of adenosine, and differs from adenosine in that the N7 of adenine is replaced by a C–H group (Fig. 1). Deaza purine nucleoside monomers have been isolated from

certain micro-organisms and are also found in nucleic acids [1]. Since these monomers are direct analogues of natural nucleosides, they can be phosphorylated and enzymatically incorporated into nucleic acid polymers. However, the presence of these analogues in nucleic acids is believed to have important structural and biochemical consequences. Research has shown that tubercidin is capable of interfering with numerous cellular processes such as purine synthesis, mitochondrial respiration, rRNA processing, methylation of tRNA, and nucleic acid

* Corresponding author.

and protein synthesis [2]. There is also considerable interest in drugs such as tubercidin for their antiviral and antitumor properties.

Since the incorporation of 7-deaza purine analogues into nucleic acids eliminates the possibility of hydrogen-bonding interactions involving the purine N7 acceptor site, this substitution has frequently been used to probe systems that may involve Hoogsteen base-pairing regimes in double-, triple-, and four-stranded nucleic acid structures [3,4]. Recently, Fletcher et al. have studied the effect of replacing adenine and guanine residues in telomeric DNA sequences by their 7-deaza analogues [5]. These telomeric sequences are believed to adopt four-stranded helical structures [6], and it is interesting to note that their results show that these substitutions cause inhibition of telomerase activity. Since telomerase inhibition may be an important strategy in cancer chemotherapy, it has been suggested that 7-deaza nucleotides may be useful for an understanding of the structural basis for telomerase activity and also for the design of telomerase inhibitors.

Despite the wide interest in structural and pharmacological aspects of DNA and RNA polymers in which purine nucleoside analogues such as tubercidin have been incorporated, there is relatively little information on the conformational changes which occur following such substitutions. A number of studies have shown that the incorporation of deoxytubercidin into alternating oligo[d(A-T)] · oligo[d(A-T)] and poly[d(A-T)] · poly[d(A-T)] sequences has a significant effect on duplex stability as measured by melting temperatures and S1 nuclease digestion [7]. In the case of the cytotoxic drug formycin, in which

the C8 and N9 atoms of adenosine have been interchanged, it has been suggested that the tendency of the nucleoside to adopt the *syn* rather than the *anti* sugar-base conformation may play an important role in determining some of its unique biological properties [8]. Studies of single-stranded homopolymers containing tubercidin have also led to suggestions that a unique conformation is adopted [9], although it is not clear that this is related to changes in the character of the glycosidic linkage, which in the crystal structure of tubercidin [10,11] is shortened by ~ 0.04 Å.

The current investigation derives from the results of previous work on poly[d(A-T)] · poly[d(A-T)]. A-T rich regions of DNA have frequently been cited as having unique structural and biochemical properties. For example, the affinity of the *lac* repressor of *E. coli* for alternating A-T regions is 100 to 1000 × greater than for random sequence DNA [12]. Transient electric dichroism studies have shown that poly[d(A-T)] · poly[d(A-T)] is approximately twice as flexible as naturally occurring random sequence DNA [13]. High-angle X-ray fibre diffraction studies have demonstrated that poly[d(A-T)] · poly[d(A-T)] is capable of adopting the D conformation of the double helix [14] in addition to the A, B and C conformations observed for natural DNA [15]. Furthermore, time-resolved X-ray fibre diffraction studies have shown that the D conformation of poly[d(A-T)] · poly[d(A-T)] can undergo a reversible humidity-driven conformational transition to the B conformation during which the pitch of the double helix changes continuously from 24 Å (characteristic of the D conformation) to 34 Å (characteristic of the

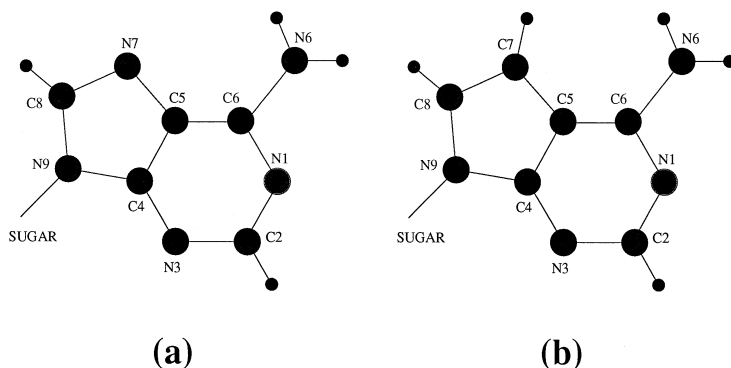


Fig. 1. The chemical structures of (a) adenine and (b) 7-deazaadenine.

B conformation) [16,17]. Since X-ray diffraction studies of oligonucleotide single crystals and X-ray and neutron fibre diffraction studies of polymeric DNA have provided a considerable amount of information on water and cation structure around the D [18], A [19–22], and B [23,24] conformations of DNA, the initial interest in performing a fibre diffraction study of poly[d(c⁷A-T)] · poly[d(c⁷A-T)] (the 7-deazaadenine analogue of poly[d(A-T)] · poly[d(A-T)]) arose from a desire to probe the significance of major groove interactions in the stabilisation of these conformations. However, any changes in DNA structure and polymorphism resulting from this substitution are also of interest in their own right since the activity of many of these nucleoside analogues may be related to these structural changes.

2. Experimental methods

2.1. Synthesis of poly[d(c⁷A-T)] · poly[d(c⁷A-T)]

Poly[d(c⁷A-T)] · poly[d(c⁷A-T)] was synthesised enzymatically by incubation of 7-deaza-2'-deoxy-

adenosine triphosphate (dc⁷ATP) and 2'-deoxythymidine triphosphate (dTTP) with DNA polymerase I. The triphosphates dc⁷ATP and dTTP were both purchased from Boehringer-Mannheim. DNA polymerase I was obtained from Promega. The synthesis was found to be highly sensitive to the concentration of triphosphates and to pH, and a number of trials were required to identify ideal conditions for high yield and a polymer length suitable for fibre preparation. A typical optimised reaction mixture used in the synthesis contained 6 mM MgCl₂, 60 mM potassium phosphate buffer (pH 6.6), 3 mM dc⁷ATP, 3 mM dTTP, 10 µg/ml poly[d(c⁷A-T)] · poly[d(c⁷A-T)] primer, 100 U/ml DNA polymerase I, 0.2 U/ml inorganic pyrophosphatase and 1 mM dithiothreitol. The reaction mixture was incubated at 37°C and polymerisation monitored by agarose gel electrophoresis. Fig. 2 shows an agarose gel illustrating the progression of the DNA synthesis during a typical reaction. The reaction was stopped by the addition of ethylenediaminetetraacetic acid (EDTA) to a final concentration of 10 mM. The efficiency of the final yield was estimated by gel filtration through Sephadex G-50 (Sigma).

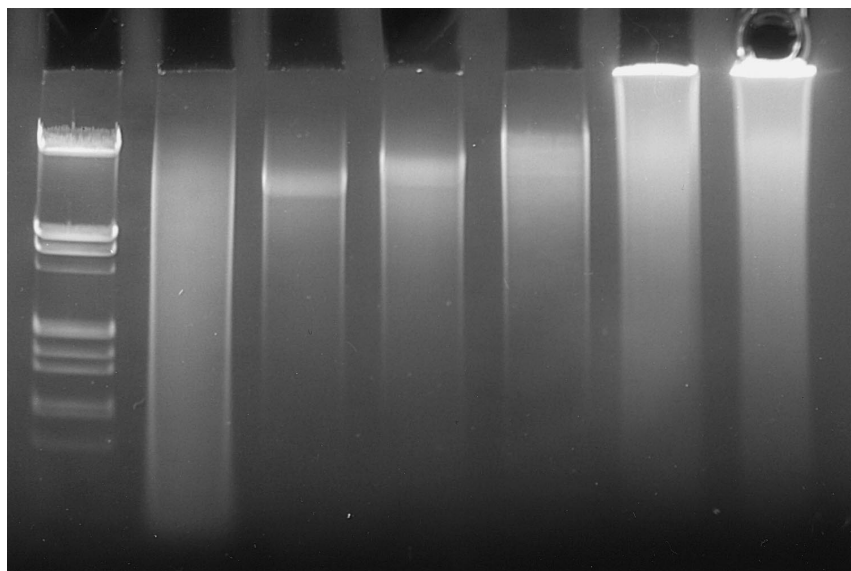


Fig. 2. The synthesis of poly[d(c⁷A-T)] · poly[d(c⁷A-T)] over a period of 41 h is clearly illustrated by this agarose gel which was stained with ethidium bromide and viewed under ultraviolet light. The first lane is a standard marker (Boehringer DNA molecular weight marker III) which contains DNA fragments of length 21,226; 5148; 4973; 4268; 3530; 2027; 1904; 1584; 1375; 947; 831; 564 and 125 base pairs (top to bottom). The second lane corresponds to the primer used and the remaining lanes from left to right show the progress of the synthesis with time. It is clear from this figure that the DNA rapidly increases in both length and concentration during the course of the reaction.

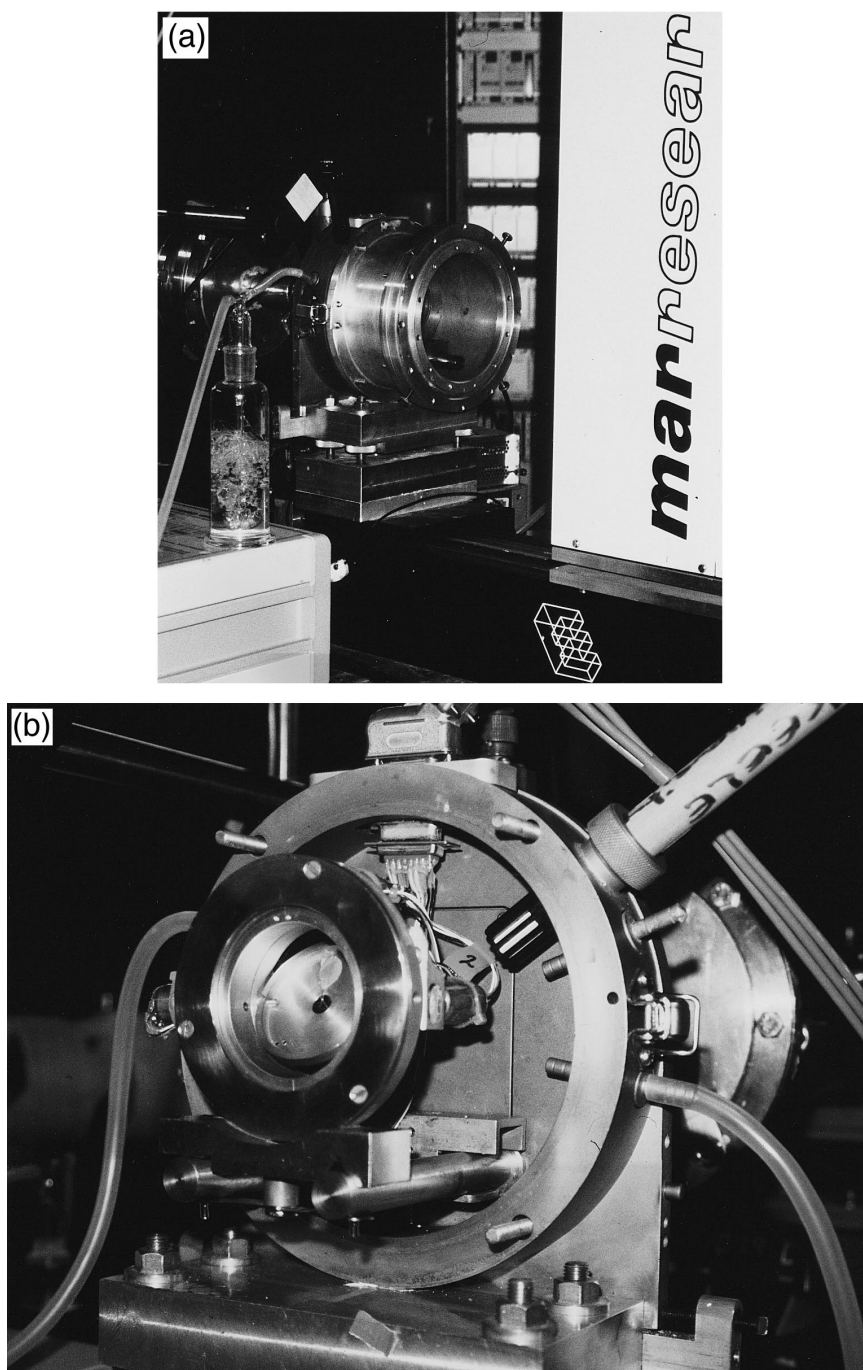


Fig. 3. (a) The X-ray high-angle fibre diffraction camera on beamline 7.2 at the SRS and (b) the motorised sample holder that allows independent control of sample position and tilt within the camera.

A nearest neighbour analysis [25] was carried out to ensure that the required alternating sequence had been synthesised. This involved an identical synthesis in which 5'-³²P-dTTP (from ICN) so that 5'-³²P-dTMP was incorporated into the polymer. The DNA was subsequently degraded to 3'-deoxyribonucleotides using micrococcal nuclease and spleen phosphodiesterase II. This process results in the transfer of the ³²P from the 5' end of dTTP before polymerisation to the 3' end of its nearest neighbour after its subsequent digestion. The digest was analysed using thin-layer chromatography in which the digestion products were detected using photographic film and compared with dAMP and dTMP standard markers. The results of this digestion study demonstrated unambiguously that an alternating A-T sequence had been synthesised in this reaction.

The DNA was purified using a mixture of phenol, chloroform, and isoamylalcohol in a 25:24:1 ratio, precipitated with cold ethanol, and pelleted by centrifugation at 8000 rpm and -10°C for 30 min. The DNA pellet was resuspended and dialysed extensively against a specific concentration of either potassium fluoride, lithium chloride, or rubidium chloride. Concentrated gels were prepared by centrifuging these solutions at 50,000 rpm for 16 h. Fibres were prepared from the gels using techniques that have been described previously [26].

2.2. Data collection

X-ray diffraction patterns were recorded using beamline 7.2 at the Daresbury Laboratory synchrotron radiation source (SRS). The configuration of this beamline has been described [27] and is optimised to exploit the similar requirements for both protein crystallography and high-angle fibre diffraction applications involving small/medium sized unit cell dimensions. The current arrangement is such that both the protein crystallography camera and the high-angle fibre diffraction camera can be mounted on the same optical bench and the changeover between the two modes of operation is trivial. Although the high-angle fibre diffraction camera was originally designed for DNA work, it is routinely used to study a wide variety of fibrous biological materials including filamentous viruses, collagen, and polysaccharides [28–30]. The camera incorporates a standard Enraf–Nonius collimator, a service collar that can be changed depending on sample requirements and monitoring methods, a sample mount system, and a melinex window that allows the passage of the scattered X-rays to the detector.

In this study, high-angle X-ray fibre diffraction patterns were recorded using a monochromatic beam of wavelength 1.488 Å and bandpass ($\Delta\lambda/\lambda$) of

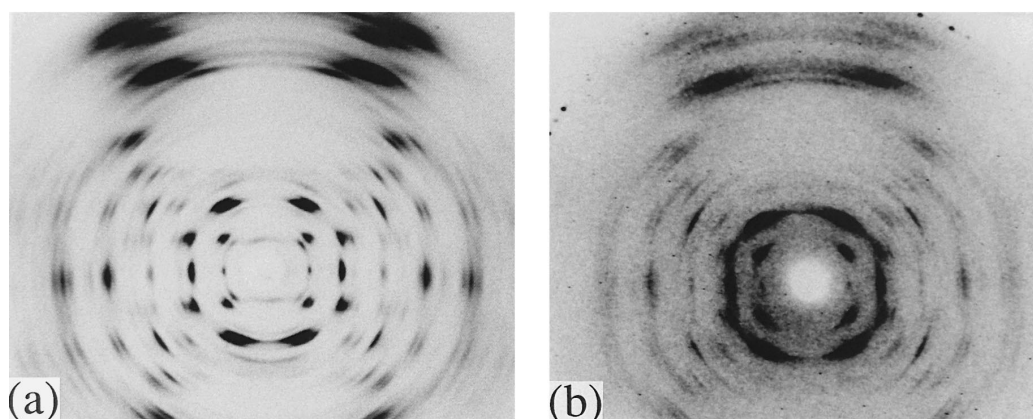


Fig. 4. (a) Diffraction pattern recorded from poly[d(c⁷A-T)] · poly[d(c⁷A-T)] using (a) the Mar Research online image plate system and (b) the Photonic Science CCD detector. Whilst the Mar image plate system provides superior spatial resolution, the CCD detector has considerable advantages in time-resolved studies.

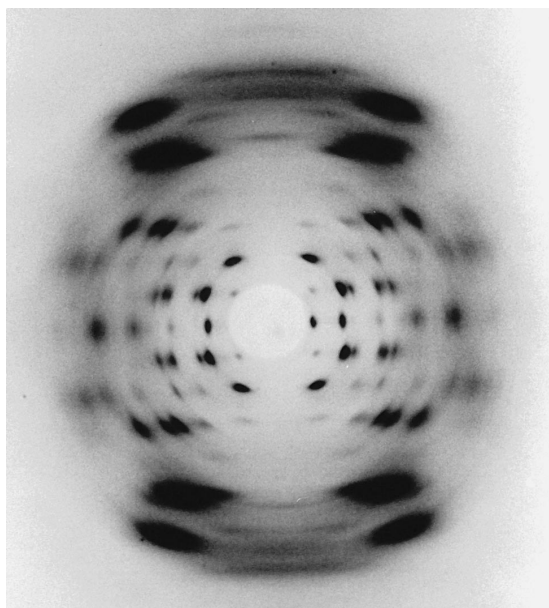


Fig. 5. The low humidity K conformation recorded from poly[d(c⁷A-T)] · poly[d(c⁷A-T)]. The pitch of the double helix is 23.5 Å.

4×10^{-4} . For all of the work described in this study (except where explicitly stated), samples were dusted with silica powder so that a calibration ring corresponding to a d-spacing of 3.138 Å was obtained. The camera interior was flooded with helium gas to minimise air scatter. The relative humidity (RH) of the fibre environment was controlled by passing the

helium gas through an appropriate saturated salt solution prior to entry into the camera. Fine control of relative humidity was obtained by adjusting the flow rate of the helium gas through the salt solution. In the work described here, the service collar accommodated a Vaisala HMP 3UT humidity probe that was used to monitor the relative humidity of the sample environment, and also provided electrical connections to a motorised sample holder that allowed the fibre position and tilt to be controlled remotely. Fig. 3 shows (a) the high-angle X-ray fibre diffraction camera used for this study and (b) the motorised sample holder. The ability to adjust the fibre tilt without disrupting the sample environment is a particularly useful feature of this experimental arrangement which fully exploits the availability of an online detecting system so that complete datasets can be recorded with essentially no ‘blind region’ in the meridional part of the diffraction data. This region of a fibre diffraction pattern arises because for a single angle of tilt, a substantial region of reciprocal space close to the [00 l] axis cannot be brought into intersection with the Ewald sphere.

Two types of area detector were used to collect diffraction patterns during these experiments. Fig. 4 shows a comparison of similar diffraction patterns recorded using the MAR Research image plate system resident on beamline 7.2 and the Photonic Science CCD system which is routinely used on this beamline by the Keele group. The MAR Research system was generally the best system to use for data

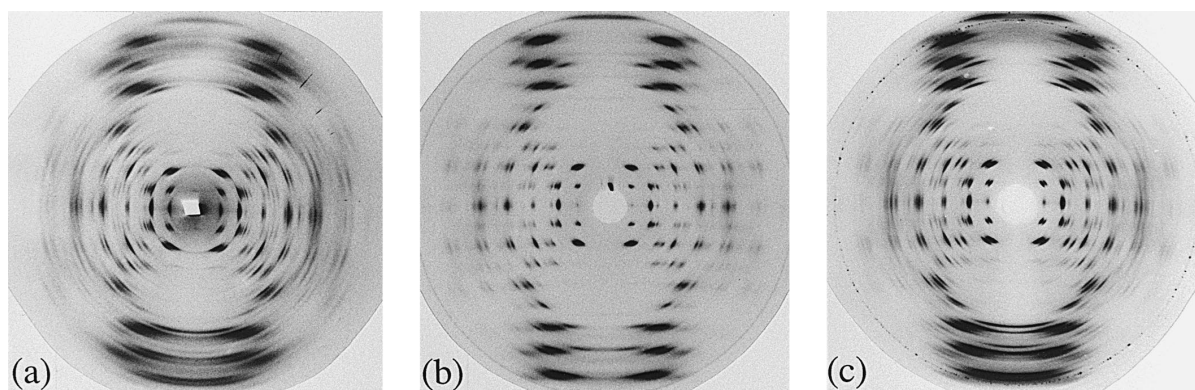


Fig. 6. Diffraction patterns recorded from the A conformation of (a) poly[d(c⁷A-T)] · poly[d(c⁷A-T)], (b) poly[d(A-T)] · poly[d(A-T)] and (c) calf thymus DNA. In (b) the continuous circle towards the outside of the pattern corresponds to a d-spacing of 3.03 Å and arises from calcite that was dusted onto the sample as a calibrant.

collection involving ‘static’ diffraction data and slow transitions. However, for real time studies of structural transitions involving rapidly-changing diffraction features, the CCD detector was more suitable, and allowed diffraction patterns to be recorded with 10 or 20 s time resolution (including a very small ‘dead-time’ of just over one second required to write the integrated data to disk). The effect of spatial

distortion in the images recorded with this detector was corrected using data from a calibration grid in conjunction with the spatial distortion correction routine of the FIT2D program [31]. One feature of the CCD system that adds considerable flexibility to the analysis procedures is that a continuous record of all data is kept on videotape, so that if necessary, integration intervals can be altered after the experiment.

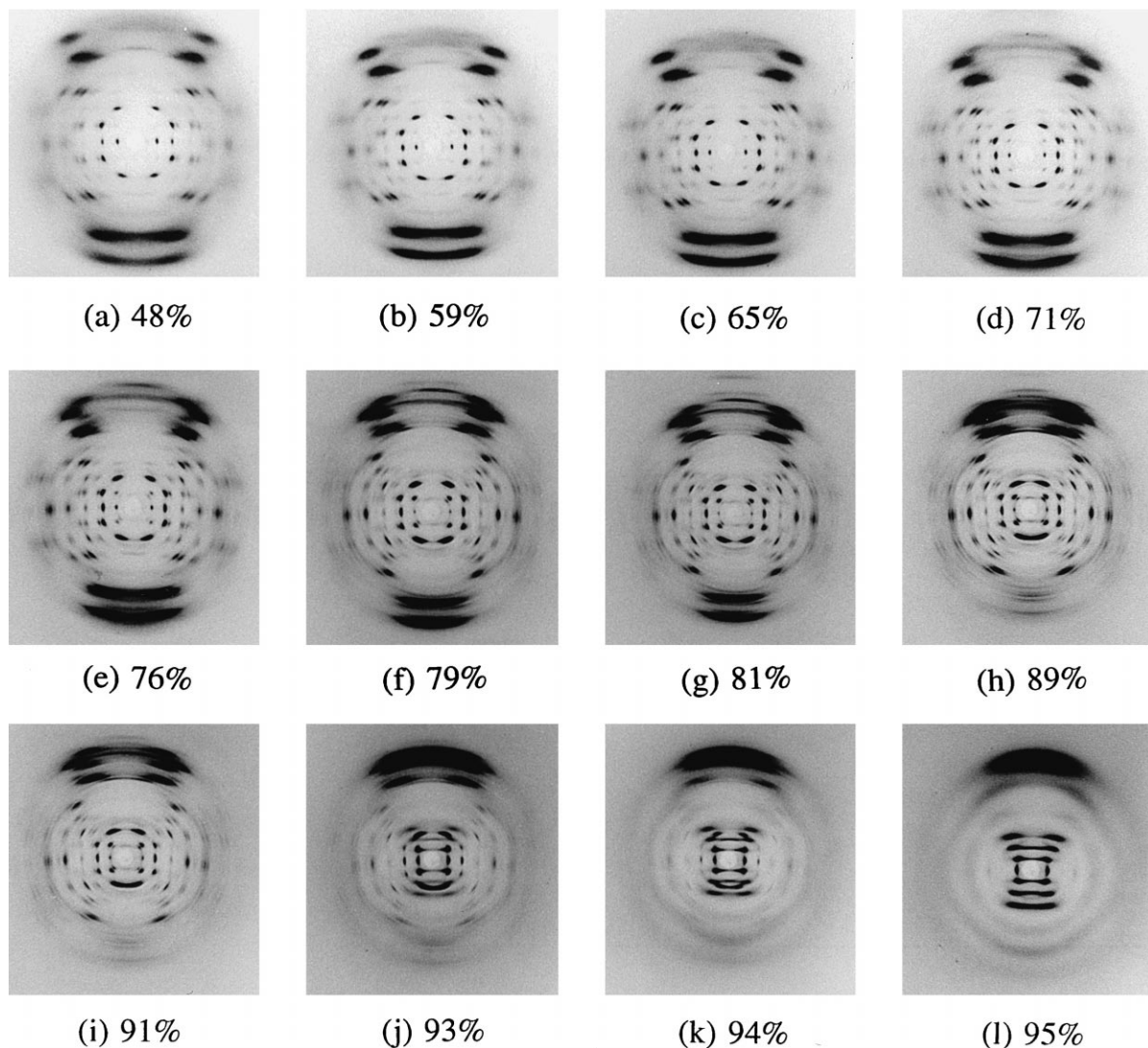


Fig. 7. The humidity driven sequence recorded using the MAR image plate detector illustrates the progress of the K to A structural transition in the relative humidity range from 48% to 76%. Beyond this the sample undergoes a structural transition to the semi-crystalline B conformation. The entire sequence from K \rightarrow A \rightarrow B is fully reversible.

2.3. Data reduction

All data reduction was undertaken using routines from the CCP13 suite of programs [32]. BSL/OTOKO file format is the standard input/output for this suite, and was used throughout this work. Where necessary, datasets were converted to this format using the program CONV. The interactive program FIX was used to determine essential pattern parameters such as image centre, specimen to detector distance, diffraction pattern rotation, and fibre tilt. The centre, rotation and tilt values obtained were refined within FIX using the ‘downhill simplex’ algorithm [33] to minimise variance between mirror related quadrants in reciprocal space. Using these refined values the image from flat film space was mapped into reciprocal space using FTOREC, and integrated intensities of Bragg reflections measured from these images using LSQINT [34].

3. Results

The presentation of the results is divided into two sections. The first section describes results recorded from samples prepared in conditions which, on the basis of previous studies [15,16], would normally favour the D conformation of the unmodified polymer. The second section deals with results recorded in conditions which favour the crystalline B conformation of the unmodified polymer. In both cases, the tubercidin derivative behaves in a very different way

from unmodified poly[d(A-T)] · poly[d(A-T)]. Despite the fact that samples were prepared for a wide range of salt strengths where the stabilising cations were Li^+ , K^+ and Rb^+ , no conditions were identified in which the D conformation was observed for the poly[d(c⁷A-T)] · poly[d(c⁷A-T)] analogue.

3.1. The observation of the low humidity ‘K’ conformation and its transition to the A conformation

In low humidity conditions which would normally favour the D conformation for the unmodified polymer, the 7-deaza analogue adopts a conformation that has not so far been described for any natural or synthetic DNA polynucleotide and which is designated here as the K conformation. The conformation has a pitch of 23.5 Å, and its diffraction pattern is shown in Fig. 5. The lattice parameters are $a = 21.9$ Å, $b = 40.3$ Å, $c = 23.5$ Å, $\alpha = 90.0^\circ$, $\beta = 97.0^\circ$, $\gamma = 90.0^\circ$.

As the relative humidity of the fibre environment is increased, this conformation undergoes a co-operative transition to a structure having lattice parameters $a = 22.7$ Å, $b = 41.1$ Å, $c = 27.5$ Å, $\alpha = 90.0^\circ$, $\beta = 97.0^\circ$, $\gamma = 90.0^\circ$ and which, despite a slightly shorter pitch, is recognisable as an A conformation. The overall intensity distribution in the inner region of the pattern is consistent with a hollow structure that has almost even strand staggering, and the diffraction observed on layer lines 6, 7, and 8 is typical of that for classical A-DNA where it is attributed particularly to the stacking of tilted base

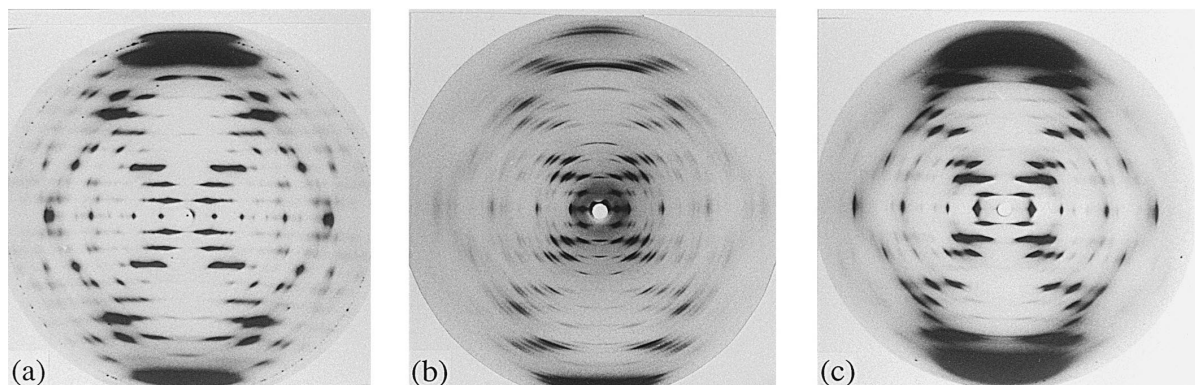


Fig. 8. The crystalline B conformation recorded from the lithium salt of (a) poly[d(c⁷A-T)] · poly[d(c⁷A-T)], (b) poly[d(A-T)] · poly[d(A-T)] and (c) calf thymus DNA.

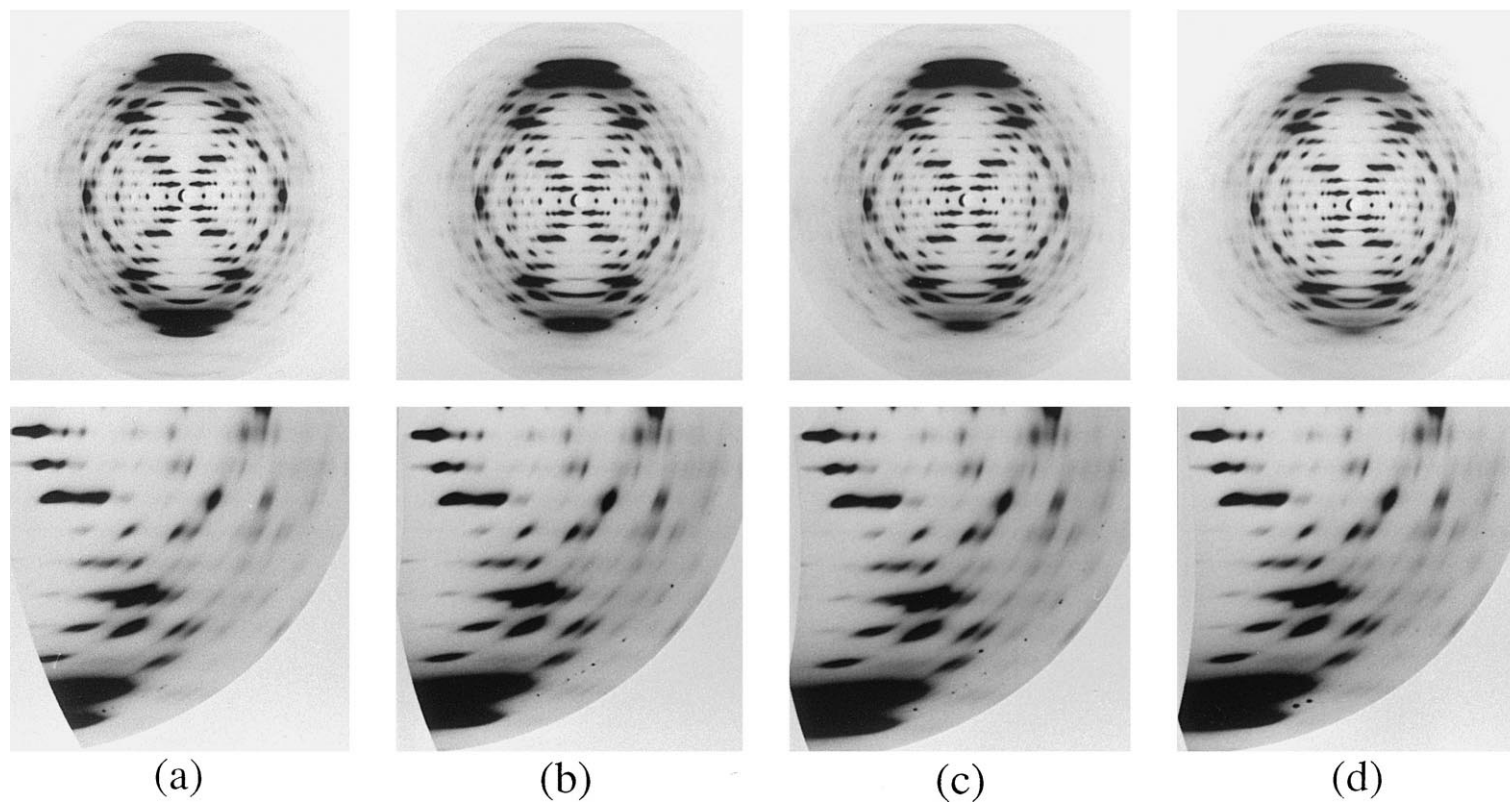


Fig. 9. Selected diffraction datasets taken from the tilt series recorded for the B conformation described in Section 3.2: (a) tilt = 0° ; (b) tilt = 7° ; (c) tilt = 10° ; (d) tilt = 12° . Each pair of images show the diffraction pattern, as recorded in flat detector space (top) and after remapping into reciprocal space (bottom). The variation of the blind region with fibre tilt angle is clear from the lower series of images.

pairs (the details of fibre diffraction data observed for A-DNA have been described in detail by Fuller et al. [35]). These features are all evident in each of the patterns shown in Fig. 6, which were recorded from the A conformations of poly[d(c⁷A-T)] · poly[d(c⁷A-T)], poly[d(A-T)] · poly[d(A-T)] and random-sequence calf thymus DNA. However, quantitative measurements have shown that subtle differences exist between the poly[d(c⁷A-T)] · poly[d(c⁷A-T)] A-DNA diffraction pattern and those recorded for the A conformations of poly[d(A-T)] · poly[d(A-T)] and random-sequence DNA, particularly in the region of the 4th, 5th and 7th layer lines of the pattern.

Fig. 7 shows a sequence of diffraction patterns recorded from a poly[d(c⁷A-T)] · poly[d(c⁷A-T)] fibre as a function of relative humidity using the online MAR image plate, and shows the transition from the K conformation to the A conformation. The pitch of the helix changes continuously from 23.5 Å (associated with K-DNA) to 27.5 Å characteristic of the A conformation of this polymer. Further increase in the relative humidity of the fibre environment results in a transition to the semi-crystalline B conformation. This same sequence of transitions was also recorded using the CCD detector. The complete CCD dataset consisted of 133 images, each collected as 20 s integrations. A structural analysis of the K conformation and of the K → A structural transition is currently in progress [36]. Both aspects of this analysis are aided by the fact that crystallinity is maintained throughout the transition, so that changes in the structure of the A conformation can be ‘traced back’ through the transition to provide an independent check of the analysis of the K conformation.

3.2. A novel B-DNA conformation from the lithium salt of poly[d(c⁷A-T)] · poly[d(c⁷A-T)]

The majority of double stranded DNA systems that have been studied by fibre diffraction adopt the crystalline B conformation in specific conditions where the stabilising cation is lithium. These diffraction patterns contain a wealth of detail and were instrumental in the first definitive structural studies of B-DNA [37,38]. In this work the lithium salt of poly[d(c⁷A-T)] · poly[d(c⁷A-T)] was therefore one of the first salts studied. The diffraction patterns

recorded were of a comparable quality to those recorded for other crystalline B conformations of natural and synthetic DNA, and demonstrated that the B conformation of this polynucleotide was also a 10-fold double helix although its pitch of 32.3 Å, was ~2.0 Å shorter than the B conformation of poly[d(A-T)] · poly[d(A-T)]. Differences in the intensity distributions observed for the B form diffraction patterns obtained from poly[d(c⁷A-T)] · poly[d(c⁷A-T)], poly[d(A-T)] · poly[d(A-T)] and random sequence calf thymus DNA are clear from a visual inspection of the patterns shown in Fig. 8. poly[d(A-T)] and random sequence calf thymus DNA. For example, the intensity distribution on layer line 2 in Fig. 8(a) is substantially weaker in relation to layer lines 1 and 3 than is the case in (b) and (c) of the same plate. Layer line 4, characteristically weak in classical B-DNA, is much stronger for the B conformation of the tubercidin analogue, and there are visible differences in the intensity distributions on layer lines 5, 6, and 7. These observations provide evidence that the B conformation of poly[d(c⁷A-T)] · poly[d(c⁷A-T)] is quite distinct in terms of strand staggering, groove depth, and base-pair orientation.

The extent of detail in the crystalline B-DNA diffraction patterns of the 7-deaza analogue meant that it was particularly important to explore a carefully chosen range of fibre tilts. The sample tilting



Fig. 10. Final dataset obtained by merging all of the diffraction patterns recorded during the tilt series. The ‘blind region’ is essentially non-existent.

system described in Section 2.2 was used to record a total of 21 exposures covering a range of tilts from 0° to 20°, in 1° intervals. Using procedures that are described by Shotton et al. [39], the individual images were binned into reciprocal space and merged to form one composite reciprocal space image in which the blind region was effectively eliminated. Fig. 9a–d shows reciprocal space images recorded for four different tilts. Fig. 10 shows the final reciprocal space image made up by merging all 21 of the diffraction datasets recorded in the tilt series. A detailed molecular modelling study of this distorted B-DNA conformation is in progress and will be reported elsewhere [36].

4. Discussion

This work demonstrates that the replacement of deoxyadenosine by deoxytubercidin has a profound effect on the conformational polymorphism in alternating A-T sequences of the DNA double helix. The structure of the B conformation is changed quite substantially in poly[d(c⁷A-T)] · poly[d(c⁷A-T)]. Additionally, no structure similar to the K conformation has been reported from previous X-ray fibre diffraction studies of natural or synthetic DNA polymers or from single crystal studies of deoxyribonucleotide oligomers. Given the wide range of conditions of salt strength and hydration that have been studied, it seems likely that the modified analogue is incapable of adopting the D conformation that is routinely observed for the unmodified polymer.

From the results described in Section 3.1, it is interesting that the A conformation is relatively unaffected by the 7-deaza substitution, and it can be expected that the small differences between the two diffraction patterns shown in Fig. 6a and b reflect rather subtle changes in helix geometry associated with the altered bond lengths and angles in the modified sugar-base conformation of deoxytubercidin residues. However, it is clear that the structures of the K and the B conformations cannot be explained in this way and it is likely therefore, that the N7/CH substitution causes disruption of DNA/water/cation interactions that are known to be of central importance in stabilising DNA conformations. In the case of the A conformation, the double helix is stabilised by a network of water

[20,22] and cations [21] in the major groove of the double helix. One of the water sites in the structure links successive O1 phosphate oxygen atoms along the same strand and may also be involved in interactions with major groove base atoms such as purine N7 [22]. Although there is no reason to suggest that the substitution of this electronegative site in poly[d(c⁷A-T)] · poly[d(c⁷A-T)] disables the O1–O1 water linkages, it is possible that the disruption of interactions between this water chain and the base-edge N7 atoms may influence the nature of structural transitions that occur as water is withdrawn from the DNA environment. The observation that the D conformation is not observed for this polymer suggests that N7 is extremely important for stabilisation of this conformation. From previous work on the location of water and ions around the D conformation [18] it is known that water/cation interactions involving the adenine N7 atom exist in the major groove and it is therefore, possible that these interactions may be vital to the stability of the D conformation.

Further interpretation of these observations will be possible when the detailed structural analyses of the K and B conformations [36] of this polynucleotide are complete. Given the dramatic structural changes in DNA conformation that result from the N7/CH substitution, it is interesting to note that biochemical studies of a number of restriction endonucleases have shown that N7 is important for both recognition and cleavage processes. In experiments where deoxytubercidin was incorporated into the DNA recognition sites of a variety of restriction endonucleases instead of deoxyadenosine, the modification inhibited the action of the enzymes [40]. Studies involving the endodeoxyribonuclease *EcoRI* have demonstrated that the replacement of deoxyadenosine by deoxytubercidin in the recognition fragment d(GAATTC) prevents cleavage [41].

The success of this study has also led to further work involving other deaza derivatives of DNA; for example, the replacement of guanine by 7-deazaguanine in polymers such as poly[d(G-C)] · poly[d(G-C)] will be valuable both from the point of view of the stereochemical requirements for the stability of the left-handed S conformation and of transitions between S-DNA and right-handed double-helical conformations [42].

Acknowledgements

We thank the BBSRC for support and Daresbury Laboratory for the provision of beamtime. We are particularly grateful for software development that has occurred as a result of the CCP13 collaborative computing project for fibre diffraction. We also thank Mike Wallace, Ted Greasley, Derek James and Graham Marsh for the construction of equipment used in this work, and Mike Davis for the construction of controller hardware. We are grateful to Elisabeth DiCapua (EMBL Outstation, Grenoble) for advice during the nearest neighbour analysis of 7-deaza DNA analogues, and to Dean Myles for technical advice during visits to beamline 7.2 at the Daresbury SRS. During this work, LHP was supported by a studentship from Keele University, MWS by an EPSRC studentship and DJH by a postdoctoral fellowship under EPSRC grant number GR/J/86643. We thank Mike Daniels for photographic work and Helen Lloyd for secretarial assistance.

References

- [1] F. Seela, A. Kehne, *Biochemistry* 24 (1985) 7556.
- [2] B.K. Hwang, B.S. Kim, *Pestic. Sci.* 44 (1995) 255.
- [3] E.W. Sayers, M.J. Waring, *Biochemistry* 32 (1993) 9094.
- [4] M. Ikehara, T. Fukui, *J. Mol. Biol.* 38 (1968) 437.
- [5] T.M. Fletcher, M. Salazar, S.F. Chen, *Biochemistry* 35 (1996) 15611.
- [6] G. Laughlan, A.I.H. Murchie, D.G. Norman, M.H. Moore, P.C.E. Moody, D.M.J. Lilley, B. Luisi, *Science* 265 (1994) 520.
- [7] F. Seela, J. Ott, D. Franzen, *Nucl. Acids Res.* 10 (4) (1982) 1389.
- [8] D.C. Ward, A. Cerami, E. Reich, *J. Biol. Chem.* 244 (12) (1969) 3243.
- [9] D.C. Ward, E. Reich, *Ann. Rep. Med. Chem.* 1969 (1970) 272.
- [10] R.M. Stroud, *Acta Cryst.* B29 (1973) 690.
- [11] J. Abola, M. Sundaralingam, *Acta Cryst.* B29 (1973) 697.
- [12] A. Klug, A. Jack, M.A. Viswamitra, O. Kennard, Z. Shakked, T.A. Steitz, *J. Mol. Biol.* 131 (1979) 669.
- [13] H.H. Chen, D.C. Rau, E. Charney, *J. Biomol. Struct. Dyn.* 2 (4) (1985) 709.
- [14] D.R. Davies, R.L. Baldwin, *J. Mol. Biol.* 6 (1963) 251.
- [15] A. Mahendrasingam, N.J. Rhodes, D.C. Goodwin, C. Nave, W.J. Pigram, W. Fuller, J. Brahms, J. Vergne, *Nature* 301 (1983) 535.
- [16] A. Mahendrasingam, V.T. Forsyth, R. Hussain, R.J. Greenall, W.J. Pigram, W. Fuller, *Science* 233 (1986) 195.
- [17] V.T. Forsyth, R.J. Greenall, R. Hussain, A. Mahendrasingam, C. Nave, W.J. Pigram, W. Fuller, *Biochem. Soc. Trans.* 14 (1986) 553.
- [18] V.T. Forsyth, A. Mahendrasingam, P. Langan, W.J. Pigram, E.D. Stevens, Y. Al-Hayalee, K.A. Bellamy, R.J. Greenall, S.A. Mason, W. Fuller, *Inst. Phys. Conf. Ser.* 101 (1990) 237.
- [19] B.N. Conner, T. Takano, S. Tanaka, K. Itakura, R.E. Dickerson, *Nature* 295 (1982) 294.
- [20] P. Langan, V.T. Forsyth, A. Mahendrasingam, W.J. Pigram, S.A. Mason, W. Fuller, *J. Biomol. Struct. Dyn.* 10 (3) (1992) 489.
- [21] P. Langan, V.T. Forsyth, A. Mahendrasingam, D. Alexeev, S.A. Mason, W. Fuller, *Proc. Ital. Phys. Soc.* 43 (1993) 235.
- [22] M.W. Shotton, L.H. Pope, V.T. Forsyth, P. Langan, R.C. Denny, U. Giesen, M.T. Dauvergne, W. Fuller, *Biophys. Chem.* 69 (1) (1997) 85.
- [23] G.G. Privé, K. Yanagi, R.E. Dickerson, *J. Mol. Biol.* 217 (1991) 177.
- [24] M.W. Shotton, L.H. Pope, V.T. Forsyth, P. Langan, H. Grimm, A. Rupprecht, R.C. Denny, W. Fuller, *Physica B*, (in press).
- [25] J. Josse, A.D. Kaiser, A. Kornberg, *J. Biol. Chem.* 236 (3) (1961) 864.
- [26] W. Fuller, F. Hutchinson, M. Spencer, M.H.F. Wilkins, *J. Mol. Biol.* 27 (1967) 507.
- [27] C. Nave, J.R. Helliwell, P.R. Moore, A.W. Thompson, J.S. Worgan, R.J. Greenall, A. Miller, S.K. Burley, J. Bradshaw, W.J. Pigram, W. Fuller, D.P. Siddons, M. Deutsch, R.T. Tregear, *J. Appl. Cryst.* 18 (1985) 396.
- [28] P. Malik, T.D. Terry, L.R. Gowda, A. Langara, S.A. Petukhov, M.F. Symmons, L.C. Welsh, D.A. Marvin, R.N. Perham, *J. Mol. Biol.* 260 (1996) 9.
- [29] T.J. Wess, A. Hammersley, L. Wess, A. Miller, *J. Mol. Biol.* 248 (1995) 487.
- [30] N.J. Fullwood, K.M. Meek, *J. Mol. Biol.* 236 (1994) 749.
- [31] A.P. Hammersley, S.O. Svensson, A. Thompson, *Nucl. Instr. Meth. Phys. Res. A* 346 (1994) 312.
- [32] R.C. Denny, *Fibre Diffraction Rev.* 5 (1996) 11.
- [33] J.A. Nelder, R. Mead, *Comput. J.* 7 (1965) 308.
- [34] R.C. Denny et al., in preparation.
- [35] W. Fuller, M.H.F. Wilkins, H.R. Wilson, L.D. Hamilton, S. Arnott, *J. Mol. Biol.* 12 (1965) 60.
- [36] L.H. Pope et al., in preparation.
- [37] R. Langridge, D.A. Marvin, W.E. Seeds, H.R. Wilson, C.W. Hooper, M.H.F. Wilkins, L.D. Hamilton, *J. Mol. Biol.* 2 (1960) 38.
- [38] S. Arnott, D.W.L. Hukins, *J. Mol. Biol.* 81 (1973) 93.
- [39] M.W. Shotton et al., in preparation.
- [40] J. Jiricny, S.G. Wood, D. Martin, A. Ubasawa, *Nucl. Acids Res.* 14 (16) (1986) 6579.
- [41] F. Seela, A. Kehne, *Biochemistry* 26 (1987) 2232.
- [42] A. Mahendrasingam, R.C. Denny, V.T. Forsyth, R.J. Greenall, W.J. Pigram, M.Z. Papiz, W. Fuller, *Inst. Phys. Conf. Ser.* 101 (1990) 225.